

# THE STABILITY OF EXOPLANETS IN THE BINARY GLIESE 86 AB

Elke Pilat-Lohinger and Barbara Funk

*Institute for Astronomy*

*University of Vienna*

*Türkenschanzstrasse 17*

*A-1180 Vienna, Austria*

lohinger@astro.univie.ac.at

**Abstract** Gliese 86 is one of 3 binary systems with a close stellar component, where an extra-solar planet was discovered. The host-star is classified as a K1 main-sequence star and its stellar companion was first identified as a brown dwarf (Els et al., 2001) and later as a white dwarf (Mugrauer & Neuhäuser, 2005). In our numerical investigation we determine the stable zone around the K1V star for different eccentricities of the binary system in both stellar configurations and compare the results of the systems. The planetary motion is analyzed by means of (a) the Fast Lyapunov Indicator (FLI) and (b) the maximum eccentricity (max-e). A study of mean motion resonances in the Gliese 86 system showed that the perturbative effects due to the discovered planet are restricted to very close orbits. Therefore, we distinguish 3 regions: (i) the *inner zone* (**IZ**), which is the region between the detected planet and the so-called habitable zone; (ii) the *habitable zone* (**HZ**) is defined as the region around a star where liquid water can exist on the surface of a terrestrial-like planet; and (iii) the *outer zone* (**OZ**) which is the region outside the HZ, which is not influenced by the detected giant planet. For the computations different dynamical models were applied – i.e. the restricted four body problem for the (**IZ**) and the **HZ**, the elliptic restricted three body problem for the (**OZ**). In general, the motion of fictitious planets in the Gliese 86 system is very stable. Only for high eccentricities of the binary ( $\geq 0.75$ ) chaotic motion occurs even in the HZ. In this case the stable zone shrinks to a small region around Gliese 86, where the eccentricity of an additional fictitious planet should be  $< 0.5$  due to perturbations of the detected giant planet.

**Keywords:** binary system: Gliese 86 – S-type orbits – stable regions – habitable zone – Fast Lyapunov Indicators – maximum eccentricity

## 1. Introduction

The discovery of extra-solar planets in binaries led to a growing interest of stability studies of such systems, where we distinguish between 2 types of motion<sup>1</sup>: the *planet (or P-) type motion* when the planet moves around both stars and the *satellite (or S-) type motion*, when the planet orbits one star. Up to now we know 14 double star systems, where planetary companions were found in S-type motion.

Dynamical studies of planetary motion in binaries were carried out during the last 25 years. There are general studies using either the three body problem (see e.g. Harrington (1977), Szebehely (1980), Szebehely & McKenzie (1981)) or the elliptic restricted three body problem<sup>2</sup> like the ones by Dvorak (1984 and 1986), Rabl & Dvorak (1988), Dvorak et al. (1989) and more recently by Holman & Wiegert (1999), Pilat-Lohinger & Dvorak (2002), Pilat-Lohinger et al. (2003) and Musielak et al. (2005). The last cited paper showed also an application to binary systems with observed giant planets, where they have chosen three systems with a close moving planet among which they selected as well Gliese 86 – which is studied in detail in the present investigation. Furthermore we have to mention that Benest studied in a series of papers several binaries numerically (see Benest 1988, 1989, 1996, 1998 and 2003).

The binary Gliese 86 is about 11 pc away from the Sun in the constellation Eridanus. The double star system consists of a K1 main sequence star ( $m_1 = 0.7M_S$ ) and in all probability a white dwarf (with a minimum mass of  $0.55M_S$ ) at about 21 AU as proposed by Mugrauer & Neuhäuser (2005) using NAOS-CONICA (NACO) and its new Simultaneous Differential Imager (SDI). The former detection by coronagraphic images using the ESO adaptive optic system ADONIS (Els et al., 2001) identified a late L or late T brown dwarf (BD) of about 50 Jupiter-masses moving at a distance of at least 18.75 AU. But Els et al. could not explain the linear trend in the observation, as it can be done by the new detection by Mugrauer & Neuhäuser (2005). However, the first who suggested a white dwarf (WD) companion for Gliese 86 was Jahreiß in 2001.

The planet is found to be very close to the K1 V star, at 0.11 AU with an orbital period of less than 16 days (Queloz et al., 2000). Due to the CORALIE measurements a minimum mass of  $4M_{\text{Jupiter}}$  was determined.

In our study we first examine numerically the dynamical behavior of fictitious low mass planets in the binary Gliese 86, where we neglect the detected planet in order to define the stable region for different eccentricities of the binary ( $e_{\text{binary}}$ ). The results for both binary configurations (i.e. BD or WD as secondary) gave rise to carry out further investigation of this double star using  $e_{\text{binary}} = 0.2$  and  $0.7$ .

Then we determine the mean motion resonances (MMRs) of the system Gliese 86 and we divide the region between the detected planet at 0.11 AU and the secondary (at 21 AU and 18.75 AU, respectively) into 3 parts: (i) the *inner zone* (**IZ**) between the detected planet and the habitable zone, where we can expect a gravitational influence of Gliese 86 b; (ii) the *habitable zone* (**HZ**), where only the inner part might be perturbed by Gliese 86 b; and (iii) the *outer zone* (**OZ**) outside the habitable zone, which is not influenced by the giant planet. The results for the different regions are discussed in sections 4 – 6.

For the computations two dynamical models are used: (i) the restricted 4 body problem<sup>3</sup> (R4BP) for the **IZ** and the **HZ**, (ii) the elliptic restricted 3 body problem (ER3BP) for the **OZ**.

Contrary to most other studies, we determine the dynamical state of the orbits not only through straightforward orbital computations but we applied a chaos indicator, with which it is easier to define the regions of long-term stability. As chaos indicator we use the Fast Lyapunov Indicator (FLI) (Froeschlé et al. 1997) and combine the results with the evolution of the orbit's eccentricity. In the next section we describe the numerical methods and the initial conditions for the computations.

## 2. Numerical setup

For the different numerical studies of the binary Gliese 86 we determine the stable zones in the orbital element space mainly by means of the fast Lyapunov Indicator (FLI). This chaos indicator measures the length of the largest tangent vector

$$\psi(t) = \sup_i \|v_i(t)\| \quad (1)$$

(where  $i = 1, \dots, n$  and  $n$  denotes the dimension of the phase space) and is therefore, a fast method to distinguish between regular and chaotic behavior. It was introduced by Froeschlé et al. in 1997. To carry out the necessary computations, we modified the n-body program<sup>4</sup> of R. Gonczi, (from the Observatory of Nice, France).

Moreover, we check the stability of the orbital motion by calculating the maximum eccentricity (max-e) (a) over the whole integration time and (b) for successive subintervals (of either 50 or 500 years<sup>5</sup>) to verify the variation of the max-e. This is an easy criterion to distinguish between regular and chaotic motion which was used e.g. by Laskar in 1994 to show the long-term evolution of the planets in the Solar System. In general it is called either *maximum action method* (see Morbidelli, 2002, p. 106) or *sup-map method* (according to Froeschlé & Lega, 1996). The computations for this study are carried out using the Lie-series method, which has also an adaptive step size control for

the correct handling of possible close encounters of celestial bodies (for details see e.g. Lichtenegger (1984) and Hanslmeier & Dvorak, (1984)).

*The initial conditions of the massive bodies* are taken from the papers by Els et al. (2001) – when the secondary  $m_2$  is a brown dwarf (BD) – and by Mugrauer & Neuhäuser (2005) – when the secondary  $m_2$  is a white dwarf (WD) – only the eccentricity of the binary ( $e_{\text{binary}}$ ) was varied (see table 1) and all angles – inclination ( $i$ ), node ( $\Omega$ ), perihelion distance ( $\omega$ ) and mean anomaly ( $M$ ) – are set to zero.

Table 1. Orbital parameters of the binary Gliese 86

	$m_1$ (K1 V star)	$m_2$ (BD)	$m_2$ (WD)	$m_3$ (planet)
mass:	$0.79 M_S$	$50 M_J$	$0.55 M_S$	$4M_J$
semi-major axis [AU]:	0.	18.75	21	0.11
eccentricity:	0.0 – 0.7	0.0 – 0.7	0.0 – 0.7	0.046

*The initial conditions of the fictitious planets* are given in table 2

Table 2. Initial conditions of the massless bodies

	orbits in the R4BP	orbits in the ER3BP
semi-major axis [AU]:	0.14 – 1. (with step: 0.01)	0.3 – 10.5 (with step: 0.01)
eccentricity:	0., 0.1, 0.2, ..., 0.5	0., 0.1, 0.2, ..., 0.5
inclination [deg]:	0	0 – 45 (with a step of 5)
$\Omega, \omega, M$ :	0	0

and the integration time for the FLI computations is between 1000 and 100000 periods of the binary, which seems to be not very much. But we have to point out that the dynamical state of an orbit can be determined with the FLIs about 200 times faster than by calculating the Lyapunov characteristic exponent (LCE)<sup>6</sup>. In addition we combine the FLI results with those of the maximum eccentricity.

### 3. General stability studies

#### 3.1 Stability of S-type motion around Gliese 86 A (without the detected planet)

Since we do not have any knowledge about the binary’s eccentricity – neither from the detection by Els et al., 2001 nor from the new observations by Mugrauer & Neuhäuser, 2005 – we study the region between the K1 V star and the secondary (BD and WD, respectively) – where we neglect the discovered giant planet – in order to define the stable zones of S-type motion around

Gliese 86 for different eccentricities of the binary ( $e_{\text{binary}} = 0$  to 0.9 with a step of 0.05). As dynamical model we use the ER3BP, where the orbital behavior is determined by (a) the application of the FLIs and (b) the max-e. The initial conditions of the Gliese 86 system are given in table 1 of section 2 (i.e.  $m_1$  and both  $m_2$ ). The massless bodies are started in circular motion at semi-major axes between 0.3 and 12 AU with a step of 0.01 AU. And the computations time is 100000 years (i.e. more than 1000 periods of the binary).

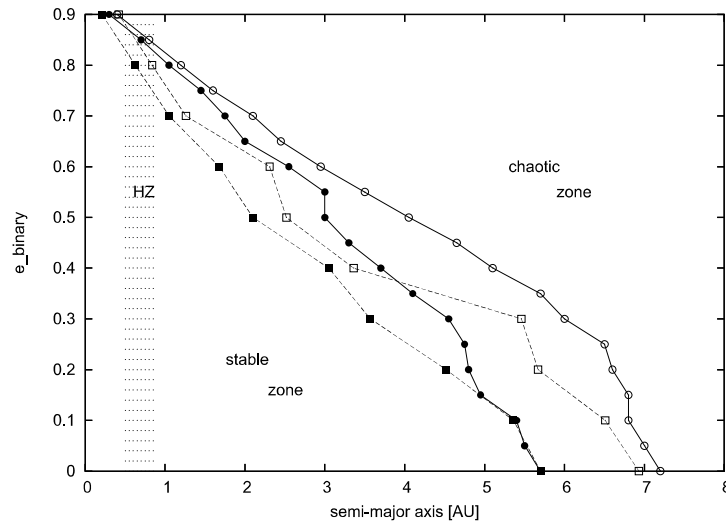


*Figure 1.* The stability of a fictitious mass-less body in the gravitational field of the binary Gliese86 AB, where the detected planet at 0.11 AU was neglected. One can see three zones (stable, mixed and chaotic) for both configurations: dashed lines with open and full squares for a WD and full lines with open and full circles for a BD as secondary.

The results of the FLI computations are shown in fig. 1 which splits the (semi-major axis,  $e_{\text{binary}}$ ) parameter space into 3 zones: (i) a *stable zone* whose border (dashed lines with black squares (for  $m_2 = \text{WD}$ )/solid line with black circles (for  $m_2 = \text{BD}$ ) is defined by the largest distance from Gliese 86 ( $= m_1$ ) up to which we have found only regular motion; (ii) a *chaotic zone*, where no regular motion can be found – which is outside the dashed line with open circles; and in-between the two border-lines one can see (iii) a *mixed zone* where both regular and chaotic motion can be found (see e.g. fig. 5.a, where these 3 zones can be clearly seen). For the old system ( $m_2 = \text{BD}$ ) one can see that the border of the chaotic zone is nearly constant up to  $e_{\text{binary}} = 0.2$  with values around 7.2 AU. An increase of the binary’s eccentricity leads to an almost linear shift of this border towards the host-star Gliese 86. Moreover, one can recognize a quit similar development of both border-lines for high eccentricities ( $e_{\text{binary}} \geq 0.65$ ), where the mixed zone is quite small. In contrast thereto, we have a large mixed zone for eccentricities up to 0.5.

For the new system ( $m_2 = \text{WD}$ ) the two border-lines show always a decrease of the stable zone and an enlargement of the chaotic zone when the binary’s

eccentricity is increased. *Remark: As a comparison we did some computations using the general three body problem with a planet's mass of about 5 Jupiter-masses. For such a system the stable zone shrinks significantly only for high eccentricity motion of the fictitious planet ( $e_{planet} \geq 0.3$ ).*

According to the results illustrated in fig. 1, we have chosen two eccentricities of the binary: (i)  $e_{binary} = 0.2$  and (ii)  $e_{binary} = 0.7$  for which we carry out further numerical studies.

### 3.2 Mean motion resonances

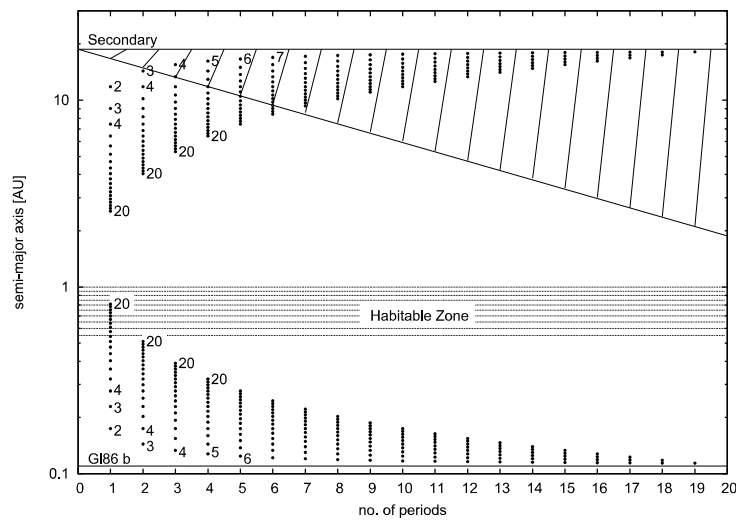


*Figure 2.* The mean motion resonances (MMRs) up to the order 20 of an additional fictitious planet with respect to Gliese 86b (lower part) and with respect to the secondary (upper part). The x-axis denotes the number of periods either for a fictitious planet (lower part) or for the secondary – BD – (upper part), and the y-axis shows the position of the resonances (on a log-scale). For a better understanding of the graphical presentation we give the following examples: e.g. "2" at  $x = 1$  and  $y = 11.14$  (upper part of the figure) means 2:1 resonance of a fictitious planet with the secondary at  $a=11.14$  AU; and "2" at  $x = 1$  and  $y = 0.174$  (lower part) means 1:2 resonance of a fictitious planet with Gliese 86b at  $a = 0.174$  AU. The hatching denotes the region which is occupied by the secondary, and since we do not have any knowledge about its eccentricity we marked this region for  $e_{secondary}$  from 0 (left border) to 0.9 (right border). The dotted region labels the habitable zone of Gliese 86. Here it is clearly seen, that the MMRs do not influence the HZ of Gliese 86 except the high order MMRs with respect to the detected planet, which are not that important. We have to note that the MMR-plot for the new system ( $m_2 = WD$ ) is quite similar to fig. 2 – so it is useless to show both.

To get a first picture about the gravitational influence of the secondary (i.e. the brown dwarf) and of the discovered planet on a fictitious planet moving in the region between these two bodies, we computed the mean motion resonances (=MMR) up to the order 20. Its representation is given in fig. 2, where the lower part is with respect to the detected planet, the upper part is with respect to the secondary and the dotted region labels the habitable zone. It is

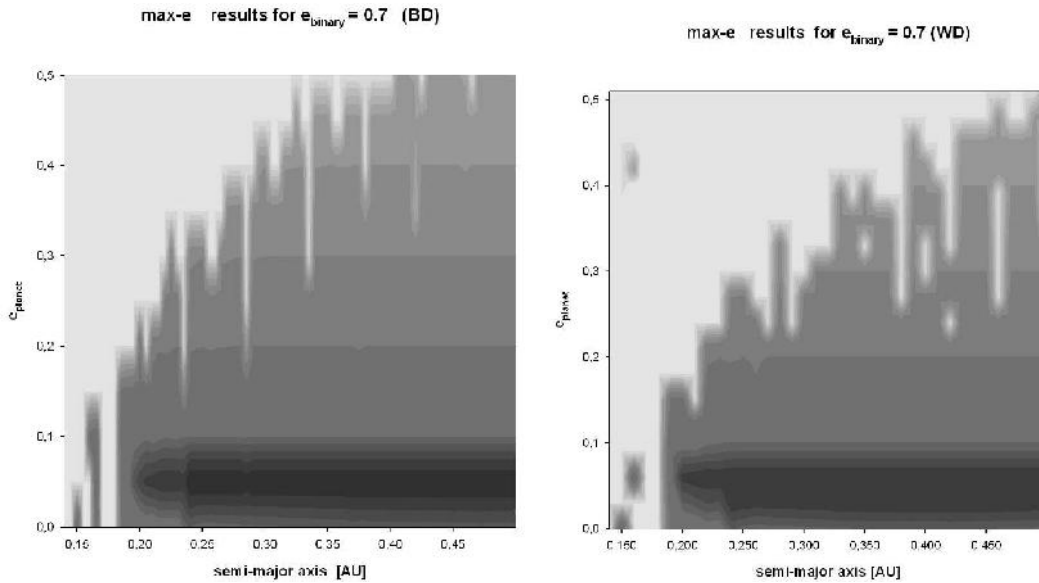


*Figure 3.* Stability maps of a fictitious massless planet in the **IZ**, where the eccentricity of this planet is varied between 0 and 0.5 and the binary’s eccentricity was fixed to 0.7 (since we expect perturbations of the secondary in the **IZ** only for high values of  $e_{\text{binary}}$ ). (a) The left panel summarizes the e-max results for the old system (BD as secondary) where the different gray shades in the stable zone indicates regions of various maximum eccentricities which increases permanently from 0.2 (black zone) around  $e_{\text{planet}} = 0.05$  to 0.6 at  $e_{\text{planet}} = 0.5$ . Additionally, one can see that initial circular motion belongs to a higher max-e level. The faintest region represents the unstable motion where the maximum eccentricity was 1. (b) The right panel is the result for the new system (WD as secondary), which shows the same overall structure. For more details see section 4.

clearly seen that most of the resonances with respect to the detected planet are concentrated to distances  $< 0.3$  AU from the K1V star and only a few, very high order resonances are in the habitable zone. Furthermore, fig. 2 explains quite well the application of different dynamical models: (i) the R4BP for the regions where we can expect an influence of the detected planet, i.e. the **IZ** and as well the **HZ**; (ii) the ER3BP for the **OZ**.

The slanted line defines the peri-center distance of the secondary for different eccentricities – from 0 (upper left position) to 0.9 (lower right position) – which indicates already an influence on the HZ for high eccentricity motion.

#### 4. The orbital behavior of fictitious planets in the inner zone

For the study of the region, where we have to expect an influence of the detected giant planet according to the MMR result, we use the R4BP and the initial conditions given in section 2 for the massive bodies. The parameter space of Gliese 86 is explored in two planes: the  $(a_0, e_{\text{binary}})$ – and in the  $(a_0, e_{\text{planet}})$ –plane<sup>7</sup>. We determine the orbital behavior by means of the FLI, which are

computed for at least 1000 periods of the binary. Low values of the chaos indicator label regular motion which is given by the dark region in fig. 3.a.

The study in the  $(a_0, e_{\text{binary}})$ -plane for circular planetary motion is not mapped since it can be described easily as the border between regular and chaotic motion is at  $a_0 = 0.19$  AU for all eccentricities of the binary. Within the chaotic region a stripe of stable motion (at  $a_0 = 0.15$  AU) for all  $e_{\text{binary}}$  was found, which is connected to the 8:5 MMR with Gliese 86b. And in the stable zone two small chaotic islands appear: one at  $a_0 \sim 0.23$  AU for  $0.2 \leq e_{\text{binary}} \leq 0.4$  (next to the 1:3 MMR) and one at  $a_0 \sim 0.206$  AU for  $e_{\text{binary}} = 0$  (close to the 2:5 MMR).

The results of a similar study for various eccentricities of fictitious planets ( $e_{\text{planet}}$ ) and a fixed eccentricity of the binary (i.e. 0.7) are given for both systems (BD and WD as secondary) in figs. 3.a and b. Comparing the two plots one can see the same overall structure: (1) An increase of the planet's eccentricity invokes as expected an increase of the chaotic region (white regions) (2) The border between regular and chaotic motion is dominated by the appearance of mean motion resonances. Which can either stabilize the motion – like at 0.15 AU for  $e_{\text{planet}} = 0$  (8:5 MMR) or at 0.16 AU for  $0.05 \leq e_{\text{planet}} \leq 0.1$  (7:4 MMR) – or destabilize the motion (faint stripes in the dark region – like the 3:1 MMR at about 0.23 AU); Both max-e plots show quite constant level-curves for the maximum eccentricity in the stable region so that we do not expect a significant influence of the detected giant planet especially on the outer part of the **IZ** for the BD secondary and at least for low-eccentricity motion of the fictitious planets in the case of a WD secondary.

## 5. The habitable zone around Gliese86 A

The HZ is roughly speaking the region around a star, where conditions similar to that of the earth can be found for a terrestrial-like planet, so that a biosphere can be built. One of the most famous work thereto was published by Kasting et al. in 1993, which is still a reference work for many studies nowadays. However, the discovery of numerous extra-solar planets<sup>8</sup> motivated scientists of different fields of research to improve the definition of the HZ based on the actual knowledge of research (Lammer et al. – ISSI project, 2005)<sup>9</sup>.

Stability studies are important contributions thereto, since long-term stability of planetary motion in the HZ is a necessary requirement for the development of a biosphere. The wideness of the HZ is limited to a small region, depending on the spectral type and the age of the host-star, therefore the planet's eccentricity has to be small enough if we require that the planet is always in the HZ.

In the case of Gliese86 A the HZ is – according to Kasting et al. (1993) – between 0.48 and 0.95 AU. As the detected gas giant moves at 0.11 AU,



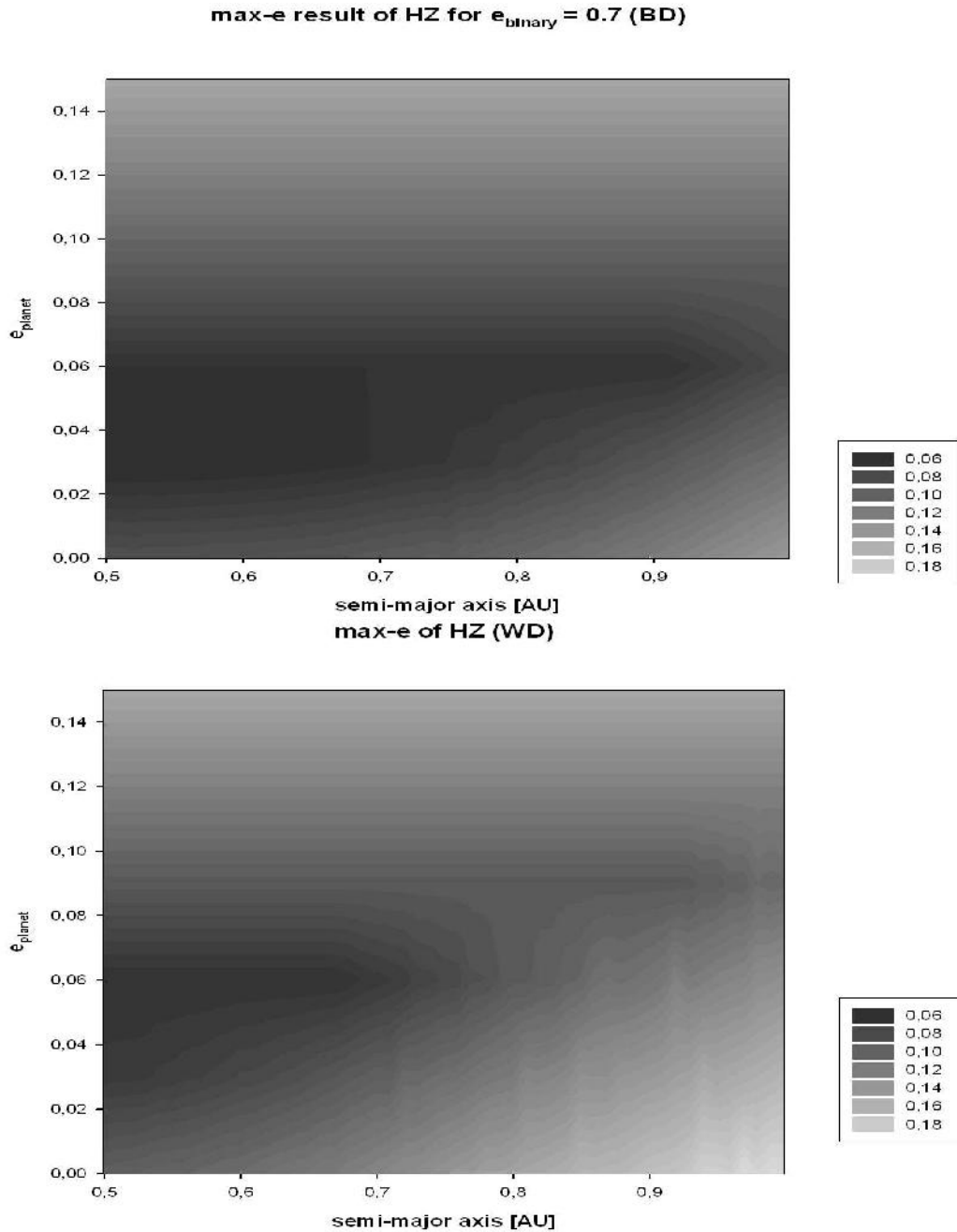


*Figure 4.* Maximum eccentricity plots of the HZ of Gliese86 A (x-axis) for fictitious planets with different initial eccentricities (y-axis) upper panel for a BD secondary and lower panel for a WD secondary. The gray shades indicate the different values of max-e, where the darkest area shows in each plot the region of highest maximum eccentricity. For more details see the text.

its gravitational influence on the HZ is not very strong, as it can be seen in fig. 2, where only high order resonances can be found in this zone. The most important question for the binary Gliese86 AB is, where was the planet built. If it was formed at a distance between 4 and 5 AU<sup>10</sup> and migrated towards the star through the HZ, an already existing terrestrial-like planet would have been

ejected from the system. But if the gas giant was built closer to the star – maybe quite near to the region, where it was found (see Wuchterl et al., 2000), then we can expect terrestrial-like planets in the HZ (which cannot be detected up to now). However, there are only a few studies that deal with the difficult problem of planetary formation in binaries (see e.g. Kley, 2001; Kley & Burkert, 2000; Nelson, 2001 or Nelson & Papaloizou, 2003), which needs still a lot of work.

Our stability study shows the HZ of Gliese 86 in a very stable state up to an eccentricity of the binary of 0.75 (for a BD secondary) an 0.7 (for a WD secondary). While for higher  $e_{\text{binary}}$  the HZ will be chaotic (see fig. 1).

In a dynamical study of the HZ it is important to control the evolution of the orbit’s eccentricity, which should be small enough so that the planet moves always in the HZ. Therefore, we show the results of the max-e study for both systems (BD and WD as secondary). As dynamical model we used the R4BP, where we studied the influence of the giant planet on a massless body in the HZ. Figs. 4.a and b summarize the results of the two systems, which show constant level lines of the max-e for initial eccentricities of the planet  $\geq 0.09$  in both plots. More precisely, the value of the max-e level curve corresponds to the initial value of  $e_{\text{planet}}$ . For lower values of the planet’s eccentricity differences can be clearly seen. However, the darkest region shows always the zone with the highest max-e value, and the “finger-like“ shape – which is different for the two systems – indicates the region of lowest e-max.

The border of the so-called “continuously habitable zone (CHZ)” (i.e. the region, where the whole planetary orbit is in the HZ) depends – from the dynamical point of view – on the initial eccentricity of the planet in the HZ. In table 3 the boundaries for the CHZ are given for different eccentricities of the fictitious planets – up to 0.33, which is the largest eccentricity for the HZ of Gliese A to find a whole planetary orbit in this zone (for higher eccentricities the CHZ would not exist anymore).

The inner boundary for circular motion is in both panels around 0.52 and the outer boundary is around 0.88 AU for the old system and about 0.83 AU in the new system. For low eccentricities of the planet it is clearly seen that the two border-lines disperse up to  $e_{\text{planet}} = 0.06$ , due to lower values of max-e, while a further increase of the planet’s eccentricity leads to an increase of the max-e value, where the two border-lines will converge. In both cases one can see the inner border at 0.565 AU and the outer border at 0.852 AU for  $e_{\text{planet}} = 0.15$ .

For a better understanding of the max-e level curves in the dynamical maps of figs. 4.a and b, we show as an example the evolution of the maximum eccentricity for an initial  $e_{\text{planet}}$  of 0.06, where the max-e value is constant (i.e. 0.06) up to a semi-major axis of 0.66 AU and increases linearly afterwards to 0.116 at 0.98 AU. In fig. 5 one can see different time evolutions of the maximum eccentricities for various initial semi-major axes of the planet (0.5 AU, 0.6 AU, 0.7 AU and 0.99 AU) where we computed the maximum eccentricity

Table 3. Boundaries for planetary motion in the HZ of Gliese 86

$e_{\text{planet}}$	inner boundary [AU]	outer boundary [AU]
0.06	0.5106	0.9245
0.07	0.5161	0.9159
0.08	0.5217	0.9074
0.09	0.5275	0.8991
0.1	0.5333	0.8909
0.11	0.5393	0.8829
0.12	0.5455	0.8750
0.13	0.5517	0.8673
0.14	0.5581	0.8596
0.15	0.5647	0.8522
0.20	0.6000	0.8167
0.25	0.6400	0.7840
0.30	0.6857	0.7538
0.33	0.7164	0.7368

for intervals of 500 years. All curves show a very regular behavior, certainly with different amplitudes and periods depending on the semi-major axis: (a) the variation of the semi-major axis from 0.5 to 0.66 AU causes a reduction of the amplitude and the period of the max-e curve (see lower 2 lines of fig. 5) and (b) on the contrary the variation of the semi-major axis from 0.67 to 0.98 AU blows up the amplitude and reduces the period of the curve (see upper 2 lines of fig. 5). This plot explains very good the difference between constant level-curves (lower 2 lines) – where the max-e value corresponds to the initial  $e_{\text{planet}}$  – and an increase of the maximum eccentricity depending on the semi-major axis (upper 2 curves).

## 6. Planetary motion in the outer zone

In figs. 6a-d we summarize the numerical results of the region outside the HZ in the two systems. As expected the more massive WD reduces the stable zone: for  $e_{\text{binary}} = 0.2$  from more than 7 AU to less than 6 AU (compare the left panels) and for a high eccentricity motion of the binary ( $e_{\text{binary}} = 0.7$ ) the border of stable motion is shifted from 2 AU to less than 1.5 AU. The most significant features of the max-e result (lower panels) are the non-dependency of the stable zone on the inclination of the planet up to about 38 deg, while higher inclinations show a decrease of the stable zone due to the Kozai resonance – which influences the whole zone at these high inclinations since we recognize an increase of the eccentricity according to the gray shades. The same behaviour was found for the new system, but the constant border

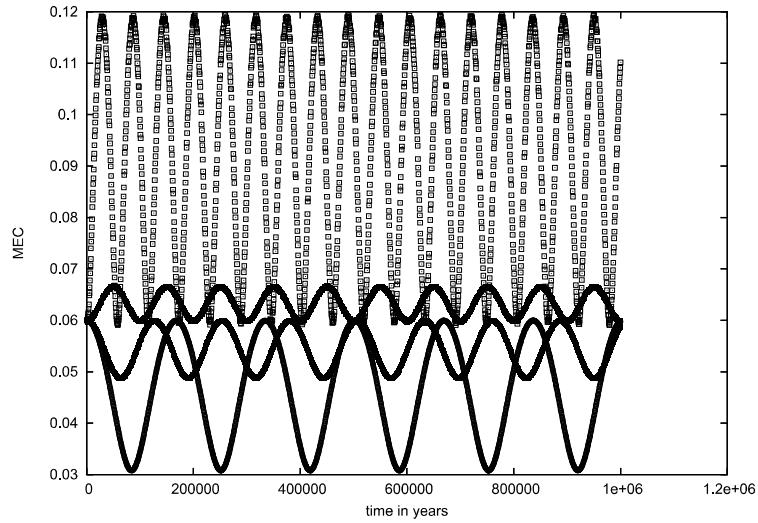


*Figure 5.* Time evolution of the maximum eccentricity for 4 different start positions of the planet: 0.5 AU, 0.6 AU, 0.7 AU and 0.99 AU, the initial eccentricity of the planet is in all cases 0.06;  $e_{\text{binary}}$  is set to 0.7 and the computation time is 1Myrs. The different behavior of the curves is described in the text (section 5).

between regular and chaotic motion is shifted to nearly 5 AU for  $e_{\text{binary}} = 0.2$  and nearly 1.3 AU for  $e_{\text{binary}} = 0.7$ .

In the upper two panels of fig. 6 one can see that an increase of the planet's eccentricity leads to a slight decrease of the stable zone as it was already found in the old system with the BD secondary (see Pilat-Lohinger et al., 2003).

## 7. Conclusion

In our numerical stability study of the binary Gliese 86 we divide the investigated region between the detected giant planet at 0.11 AU and the secondary (a white dwarf at about 21 AU or a brown dwarf at about 18.75 AU) into 3 zones:

(i) **IZ** – inner zone – is the region from 0.14 to 0.48 AU which is influenced gravitationally by the giant planet, mainly by mean motion resonances, which can stabilize or destabilize the region.

(ii) **HZ** is the habitable zone, which is from the dynamical point of view very stable for this system, especially for weakly eccentric motion of the binary. From the 3 cases of HZ:

- 1 the HZ is between the host-star and the detected giant planet,
- 2 the giant planet moves in the HZ,
- 3 the HZ is outside the discovered giant planet,

that we can distinguish from the observations for dynamical studies, Gliese 86 A is an example for the third case. As a consequence we can

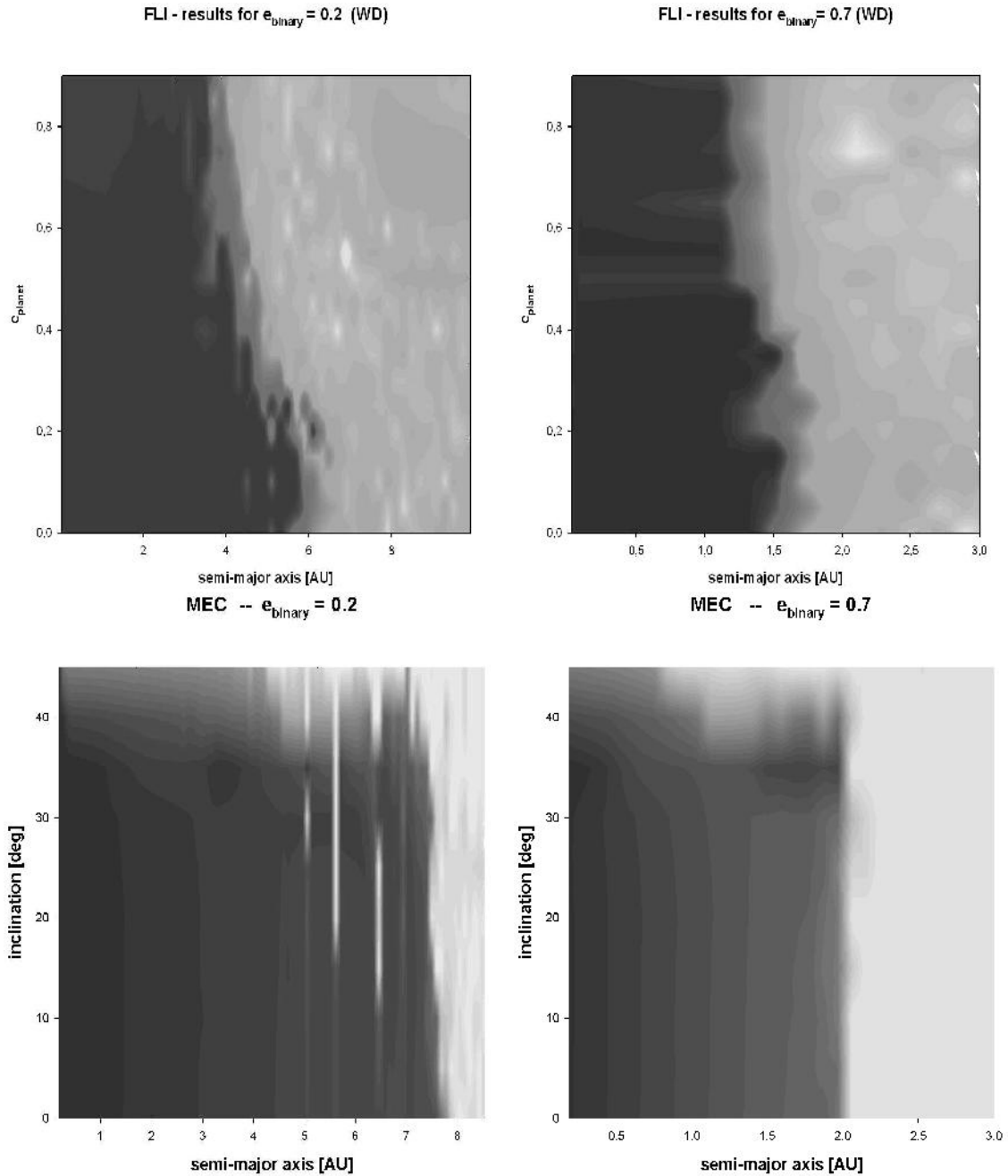


Figure 6. Stable zone for planetary motion in the binary Gliese 86 AB: the upper two panels show the results of FLI computations in the new system (the WD secondary) and the lower two panels show the e-max results of the old system (the BD secondary). The eccentricity of the binary is 0.2 for the left panels and 0.7 for the right panels. The stable motion in the (a,i)- or (a, $e_{\text{planet}}$ )-plane is given by the dark region in all plots. Please note the different scaling for the figures.

say, it has from the dynamical point of view a high probability of hosting an Earth-like planet in the habitable zone, as it was also found in the study by Menou and Tabachnik (2003).

But for such systems the most important question is, where the giant planet was built – at or beyond 5 AU or closer to the position, where it was found – but this cannot be answered by pure dynamical studies. Although if the FLI result shows the HZ fully stable, an additional max-e study is necessary to define the dynamical continuously habitable zone (CHZ), within which the fictitious planets remain all the time.

However, we have found that even for an eccentricity of 0.7 of the binary the whole HZ of Gliese 86 is stable.

- (iii) **OZ** – outer zone – is the outermost region, where the detected planet has no influence, so that the stable zone depends only on the mass-ratio and the eccentricity of the binary. A comparison of the old (the BD secondary) and the new system (the WD secondary) shows the expected decrease of the stable zone in the new system due to the higher mass of the secondary.

In a future work we will use this binary to study the influence of a hot-Jupiter on the HZ in detail.

## Acknowledgments

The authors want to thank especially Dr. M. Endl from the McDonald Observatory for many fruitful discussions about Gliese 86. EP-L wishes to acknowledge the support by the Austrian FWF (Hertha Firnberg Project T122). BF wishes to acknowledge the support by the FWF project P16024. This study was also supported by the International Space Science Institute (ISSI) and benefits from the team ‘Evolution of Habitable Planets’. The support of the Austrian-Hungarian Scientific and Technology Cooperation, grant number A-12/04 is also acknowledged.

## Notes

1. According to Dvorak (1986) there are 3 types of motion in binary systems but since the libration- (or L-)type motion is limited to certain mass-ratios of the two massive bodies ( $\sim 1/25$ ), studies of binary systems can be restricted to the S-type and P-type motion.
2. The elliptic restricted three body problem studies the motion of a massless body moving in the gravitational field of two massive bodies, which move in Keplerian orbits around their center of mass.
3. In the restricted four body problem we study the motion of a massless body in the gravitational field of the primary ( $= m_1$ ), the secondary ( $= m_2$ ) and the giant planet ( $= m_3$ )
4. The program of R. Gonczi applies the Bulirsch-Stoer method for the orbital computations and determines also the Lyapunov Exponent in its original version.
5. The time interval for the maximum eccentricity depends on the chosen integration time.
6. private communication with C. Froeschlé and E. Lega
7.  $a_0$  is the initial semi-major axis of a fictitious planet;  $e_{\text{binary}}$  is the initial eccentricity of the binary and  $e_{\text{planet}}$  is the initial eccentricity of a fictitious planet.

8. Due to the observational techniques all detected planets are gas giants - but hopefully the planned space missions (like COROT, Darwin, TPF, ...) will find terrestrial-like planets in the HZ of other sun-like stars

9. An ongoing project supported by the International Space Science Institute in Bern, Switzerland

10. Before the discovery of extra-solar planets it was claimed by A. Boss that the formation of gas planets is at or outside 5 AU (which is called snow-line).

## References

- [1] Benest, D. 1988, *A&A* **206**, 143
- [2] Benest, D. 1989, *A&A* **223**, 361
- [3] Benest, D. 1996, *A&A* **314**, 983
- [4] Benest, D. 1998, *A&A* **332**, 1147
- [5] Benest, D. 2003, *A&A* **400**, 1103
- [6] Dvorak, R. 1984, *CMDA* **34**, 369
- [7] Dvorak, R. 1986, *A&A* **167**, 379
- [8] Dvorak, R., Froeschlé, Ch. Froeschlé, C. 1989, *A&A* **226**, 335
- [9] Els, S.G., Sterzik M.F., Marchis F., Pantin E., Endl M., Kürster M. 2001, *A&A* **370**, L1–L4
- [10] Froeschlé, C., Lega, E., Gonczi, R. 1997, *CMDA* **67**, 41
- [11] Froeschlé, C., Lega, E. 1996, *CMDA* **64**, 21
- [12] Hanslmeier, A., Dvorak, R. 1984, *A&A* **132**, 203
- [13] Harrington, R.S. 1977, *AJ* **82**, 753
- [14] Holman, M.J., Wiegert P.A. 1999, *AJ* **117**, 621
- [15] Jahreiß, H. 2001, *Astronomische Gesellschaft Abstract Series* **18**,#P110
- [16] Kasting, J.F. 1993, *Icarus* **101**, 108
- [17] Kley, W. 2001, *IAUS in Potsdam 2000*, eds. H. Zinnecker and R.D.Mathieu,511
- [18] Kley, W., Burkert, A. 2000, *ASP Conference Proceedings* **219** eds. F. Garzoñ, C.Eiroa, D.de Winter and T.J.Mahoney Astron.Society of the Pacific, 189
- [19] Laskar, J. 1994, *A&A* **287**, 9
- [20] Lichtenegger, H. 1984, *CMDA* **34**, 357
- [21] Menou, K., Tabachnik, S. 2003, *ApJ* **583**,473
- [22] Morbidelli, A. 2002, *Modern Celestial Mechanics, Aspects of Solar System Dynamics* Taylor & Francis, London, 106
- [23] Musielak, Z.E., Cuntz, M., Marshall, E.A., Stuit, T.D. 2005, *A&A* **434**, 355
- [24] Nelson, R. 2001, *Astronomische Gesellschaft Abstract Series* **18**
- [25] Nelson, R., Papaloizou J.C.B. 2003, *Proceedings of the DARWIN/TPF conference in Heidelberg 2003* ESA Publications Division, ISBN 92-9092-849-2, 175
- [26] Pilat-Lohinger, E., Dvorak, R. 2002, *CMDA* **82**, 143
- [27] Pilat-Lohinger, E., Funk, B., Dvorak, R. 2003, *A&A* **400**, 1085
- [28] Pilat-Lohinger, E., Dvorak, R., Funk, B., Bois, E., Freistetter, F.: 2003, *Proceedings of the DARWIN/TPF conference in Heidelberg 2003* ESA Publications Division, ISBN 92-9092-849-2, 543

- [29] Queloz, D., Mayor, M., Weber, L., Boucha, A., Burnet, M., Confino, B., Naef, D., Pepe, F., Santos, N., Udry, S. 2000, *A&A* **354**, 99
- [30] Rabl, G., Dvorak, R. 1988, *A&A* **191**, 385
- [31] Szebehely, V. 1980, *CMDA* **22**, 7
- [32] Szebehely, V., McKenzie, R. 1981, *CMDA* **23**, 131
- [33] Wuchterl, G., Guillot, T., Lissauer, J.J. 2000, in *Protostars and Planets IV* eds. V. Mannings, A.P. Boss and S.S. Russell Univ. of Arizona Press, 1081